A NEW CHEMICAL REMEDIATION PRODUCT TO PREVENT SAND PRODUCTION FROM UNCONSOLIDATED POROUS MEDIA

B. Marchand[1,2], C. A. Davy[1,2], F. Agostini[1,3], F. Skoczylas[1,3], A. Lange[4], L. Jeannin[4], P. Egermann[4]

Affiliations:
1: Ecole Centrale de Lille, CS 20048, F-59651 Villeneuve d'Ascq, France
2: UCCS UMR CNRS 8181, F-59650 Villeneuve d'Ascq, France
3: LAM3, F-59650 Villeneuve d'Ascq, France
4: Storengy, Centre d'Expertise, 12 rue Raoul Nordling, 92274 Bois-Colombes, CS 70001, France

This paper was prepared for presentation at the International Symposium of the Society of Core Analysts held in Trondheim, Norway, 27-30 August 2018

ABSTRACT

A new chemical remediation product to prevent sand production in unconsolidated formation is studied. This binder shows a similar strengthening to that of common binder such as PAM (PolyAcrylaMide) and does not induce permeability decrease. Moreover, its performance is not reduced by water injection; it is thus a good candidate to prevent sand production.

INTRODUCTION

Unconsolidated porous media are subjected to in situ stress variations during the reservoir lifetime. This may induce progressive sand production [1], leading to delivery rate limitations and potentially premature ageing of both the downhole and the surface equipments.

In this contribution, we investigate a chemical consolidation process in the context of natural gas storage, which is complementary to the standard mechanical techniques (screen, gravel pack) [2]. The chemical binder is either mineral [3], resin-based [4] or polymer-based [5-7]. Chemical solutions are a compromise between rock reinforcement and gas permeability reduction, although they do not resist after about five years use, and they are rendered useless by the presence of underground water. Mechanisms of the reinforcement by polymer solutions has been investigated in [8]. The proposed innovative grain binder (or Novel Binder NB) aims at improving the strength and durability of the consolidation process, compared to existing polymer-based solutions. The principle of the chemical process itself remains standard, with a liquid binder (cement grout), injected into the porous medium to promote chemical reactions in inter-grain locations, leading to consolidation. The main challenge is to avoid permeability alteration. This is achieved by flushing the chemical product towards a residual value, before it reacts, so that it binds only as pending rings at the inter-grain locations.

In this study, different binders are tested, a reference one, composed of a water solution of PolyAcrylaMide (PAM), already used at the industrial scale, and seven innovative solutions labelled SB, A, B, C, D, E and F (patent pending). The porous medium is a model material made of siliceous sand with a normalized particle size distribution. At the centimetric scale, tubes of compacted sand are used to obtain similar characteristics (porosity, permeability, Pore Size Distributions i.e. PSD) to the *in situ* porous media. Binders are injected using a syringe, and then flushed towards residual saturation value using compressed air. For each tube, the consolidation pressure and gas permeability for various maturation durations are measured by using an original fluidization set-up. Argon passes through the tube, until gas flow stabilizes under increasing gas pressure (it is the so-called fluidization stage), or until sample failure in the case of important consolidation. The experience consists in increasing the gas flowrate (from 1 to 15 ln/min) step by step every minute, and measuring the corresponding upstream pressure. In parallel, gas permeability is measured continuously.

MATERIALS AND METHODS

Materials

Thirteen *in situ* sandstone samples have been retrieved from an actual industrial reservoir rock by Storengy and used throughout this work. Their shape, size, and grain size are variable, depending on the reservoir unit (fluviatile deposit context).

Because the number of real samples was limited, analogues compacted sand samples have been prepared and used for injection of NB, flushing, maturation and fluidization. A standard grain size siliceous sand (EN196-1) from Leucate (France) is used. It is compacted in a plastic tube of 10 mm diameter. The tube is closed at each end by plastic plugs. Each plug has a central hole of 3 mm inner diameter allowing injection and flushing. The sand is poured in the tube (closed on its bottom end) until it is filled. Compaction is performed by applying a pressure on the sand with the upper plug (by descending it inside the tube). At the same time, the side of the tube is gently tapped with a steel spatula, until the top edge of the upper plug comes in contact with the end of the plastic tube, and no sand comes through the 3mm hole of the lower plug. Whenever sand still comes out after the edge of the upper plug is in contact with the plastic tube, the upper plug is removed, and more sand is added. Compaction is done once more until no more sand comes out of the tube at the end of the process. The sand height is 3.17 cm ± 0.3 cm.

Methods

Hydrostatic Weighing

This method to measure porosity is used for the *in situ* sandstones. All samples are preliminarily oven-dried at 105°C until their mass is stable. By this process, we obtain their dry mass m_{dry}. The samples are then liquid-saturated, by immersion in ethanol placed inside a hermetic chamber, where partial vacuum is applied above the liquid. Full saturation is achieved when sample mass is stable. Its saturated mass is then m_{sat}. By definition, the pore volume is then: $V_p = (m_{sat} - m_{sec})/\rho_{eth}$, were ρ_{eth} is liquid ethanol density (0.789 g/cm^3 at 20°C). After liquid saturation, all samples are weighed while still immersed in ethanol. The

hydrostatic method provides m_{imm}, which is equal to (m_{sat} - ρ_{eth} V_t), where V_t is sample volume. Porosity Φ is then calculated by the following formula:

$$\Phi = V_p/V_t = (m_{sat} - m_{sec})/ (m_{sat} - m_{imm}) \quad (1)$$

Compacity Measurement

This method to measure porosity is used for the sand samples compacted in plastic tubes (see above), because they are difficult to saturate without exceeding the sample boundaries, and the sand intrinsic density ρ_s is well known (ρ_s = 2.6 g.cm^{-3}). First, the mass of the sand sample is measured (m_{sand}). Then, the apparent volume occupied by the sand, noted V_{sand}, is measured by weighing the mass of a tube full of water (m_w), considering water density ρ_w, as: $V_{sand} = V_w = m_w / \rho_w$, where V_w is water volume. Compacity C is then calculated as: $C = m_{sand}/V_{sand}$. Finally, porosity is given by: $\Phi = 1 - C$.

Mercury Intrusion Porosimetry (MIP)

MIP was performed on a Micromeritics AutoPore IV 9500 V1.03 apparatus, with the following settings: advance contact angle = 130 °, Hg surface tension = 485 dynes/cm, Hg density = 13.5335, evacuation pressure = 50 µmHg, evacuation time = 5 mins, mercury filling absolute pressure = 3,1 kPa, equilibration time = 20 s, and pressure range from 0 to 228 MPa.

X-Ray Micro-Computed Tomography (micro-CT)

A sample of compacted sand (in a plastic tube) is impregnated with epoxy resin. After resin polymerization, several rods of 2x2x10 cm are cut with a diamond saw. The rods are imaged by a X-Ray Micro-Computed Tomograph (Ultratom, RxSolution). The sample voxel size is 1.062 µm^3.

Image processing is performed using the ImageJ software (version 1.51h under Java 1.8.0_111 in 64bit). The plugin CLAHE is used to enhance contrast, the plugin Anisotropic Diffusion 2D is used as noise reducer, and the threshold algorithm Huang is selected to binarize the images (pores in white and sand grains in black). Porosity is calculated in 2D, over all the microCT images, by dividing the white pixel number (pores) by the black pixel number (sand grains). The grain size distribution is obtained using the MIP simulation tool of the Beat plugin (made available at ftp://ftp.empa.ch/pub/empa/outgoing/BeatsRamsch/lib [10]). MIP simulation is performed along six main intrusion directions (i.e. by starting from any of the six boundary surfaces of the 3D micro-CT sample).

Injection, flushing and maturation

Each compacted sand sample is subjected to an injection of one of the chemical binders. It is then flushed and cured (matured) at given temperature before the fluidization test, which aims at determining the binder performance. The injection and flushing procedure is derived from [8]. A volume of 10ml binder is injected with a graduated syringe through the sand sample. Then, flushing is performed with laboratory compressed air for 20s. Three different maturation methods (labelled m1, m2 and m3) are tested after injection:

- m1: Flushing is performed right after the injection. The sample is placed for 24h in an oven at 70 °C, and then 6 days at 20 °C before fluidization.
- m2: Before flushing, the sample is placed for 24h at 70 °C. It is flushed and then placed for 7 more days at 70 °C before fluidization.
- m3: Before flushing, the sample is placed for 24h at 20 °C. It is flushed and then placed for 7 days at 20 °C before fluidization.

The mass of the consolidated sand sample is weighted after injection (m_i), after the first 24h cure (m_c), after flushing (m_f) and just before fluidization (m_{f2}).

Fluidization

The fluidization experiment [8] consists in (1) flowing argon gas through a granular medium (here, the consolidated sand) at given flowrate and (2) measuring the corresponding gas pressure. Its outputs are the maximum gas pressure P_{max} sustained by the consolidated sand, as a measurement of its strengthening, and gas permeability K_{gas} as a measurement of gas production ability.

Gas flowrate is initially fixed at 1 ln/min and then increased step wisely by 1 ln over one minute, stabilized for one min and increased again by 1ln/min, stabilized for one minute, and so on until reaching 15 ln/min. Maximum gas pressure and flowrate are those at the first damage of the sample (corresponding to its failure), or when the experiment reaches it limits (flowrate of 15 ln/min or gas pressure of 0.5 MPa).

Strengthening is measured with and without water injection through the consolidated sand medium. If there is no water injection, the plugs at the tube ends are taken off just before fluidization. Otherwise, a volume of 10 ml of tap water is injected with a graduated syringe through the sample, then flushed with laboratory compressed air during 15 s. The tube end plugs are then removed to perform fluidization. In both cases, after plug removal, sample length L is measured with a caliper.

As high flowrates (on the order of 1ln/min) are applied, gas permeability K_{gas} (in m²) is calculated with Forchheimer's equation [9]:

$$\nabla P = -(\mu/K)(Q/S) + \beta\rho(Q/S)^2 \quad (3)$$

where ∇P is gas pressure gradient between the sample ends (in Pa), μ is argon gas dynamic viscosity (in Pa.s), Q is volumetric flowrate (in $m^3.s$), S is sample cross sectional area (in m²), ρ gas density (in $kg.m^{-3}$) and β Forchheimer coefficient (m^{-1}). In practice, ∇P is plotted as a function of Q, in order to determine Forchheimer's coefficient. Interpolation by a parabolic curve provides Pearson's correlation coefficients above 90%.

RESULTS AND DISCUSSION

Porosity

In situ sandstone and compacted sand porosity are compared as average, minimum and maximum values in Fig. 1. The porosity values for the sandstone ranges from 15.5 % to 28.7 %. It is wider than for compacted sand (26.5 % to 28.5 %). However, compacted sand porosity ranges within the highest porosity values measured for the *in situ* sandstone, which are the facies more prone to sand production. It is then concluded that compacted sand is a good analogue from a porosity perspective.

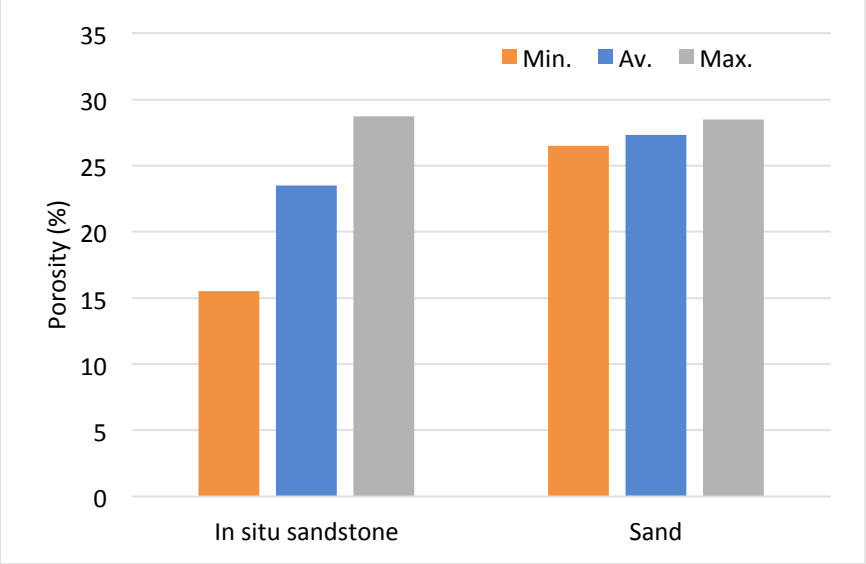

Figure 1. Porosity values (minimum, average and maximum values) for 13 in situ sandstone samples and 5 compacted sand samples.

Pore size distributions (PSD)

PSD are compared for six *in situ* sandstone samples and one compacted sand sample (Fig. 2). PSD are wider for in situ sandstone than for compacted sand, with values from 0.01 µm to 400 µm (sandstone) and from 2 µm to 80 µm (compacted sand). However, for compacted sand, resolution is limited to 1 µm (micro-CT voxel size), so that smaller pores than those determined here may exist. The sandstone sample displaying the smallest pore sizes contains clay and, in this contribution, it is assumed that they are not representative of the reservoir rock for gas storage. They are not taken into account in the comparison with compacted sand.

Considering d_{10} (i.e. the pore size corresponding to 10% of the PSD), compacted sand has a six times higher value than sandstone. Considering d_{50} (50% of the PSD), compacted sand is within the range of d_{50}(sandstone). Considering d_{90} (90% of the PSD), d_{90}(sand) is at least 1.5 time smaller than d_{10}(sandstone). The PSD of sand is therefore narrower and with generally smaller pores than *in situ* sandstone. It consists nevertheless on a fair analogue of the PSD of the less consolidated reservoir samples.

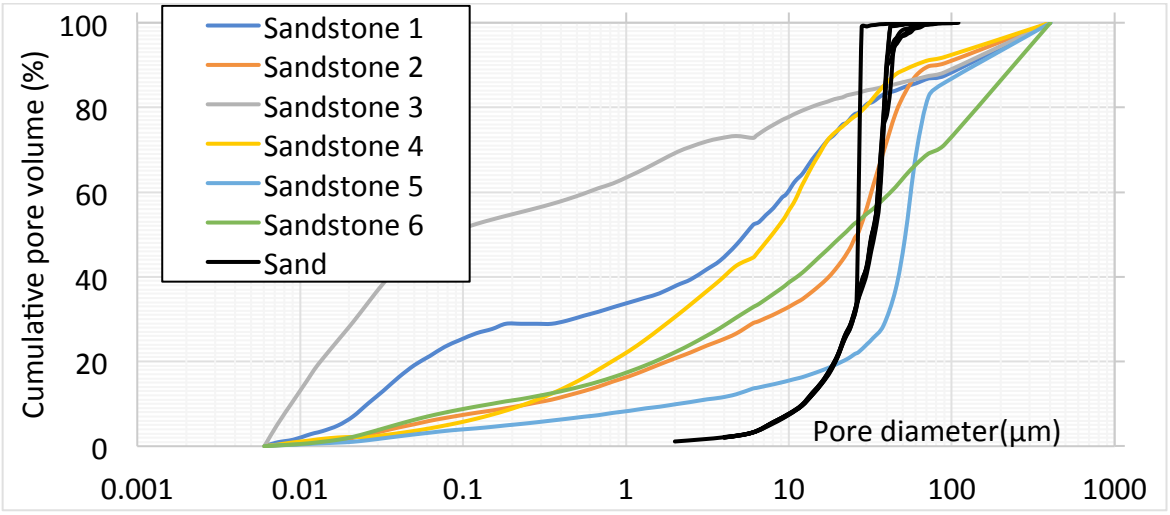

Figure 2. Pore size distribution of 6 in situ sandstone samples and one compacted sand sample. For the sand, the six directions of intrusion of MIP simulation are represented.

Fluidization

Figure 3 shows maximum gas pressure P_{max} and gas permeability K_{gas} for PAM and new chemical binders SB, A, B, C and D after m1 maturation process, with and without water injection before fluidization. For one of the four samples consolidated with PAM maximum gas pressure is a failure pressure; for the others samples, maximum gas pressure is the pressure at 15 ln/min without measurable sample failure.

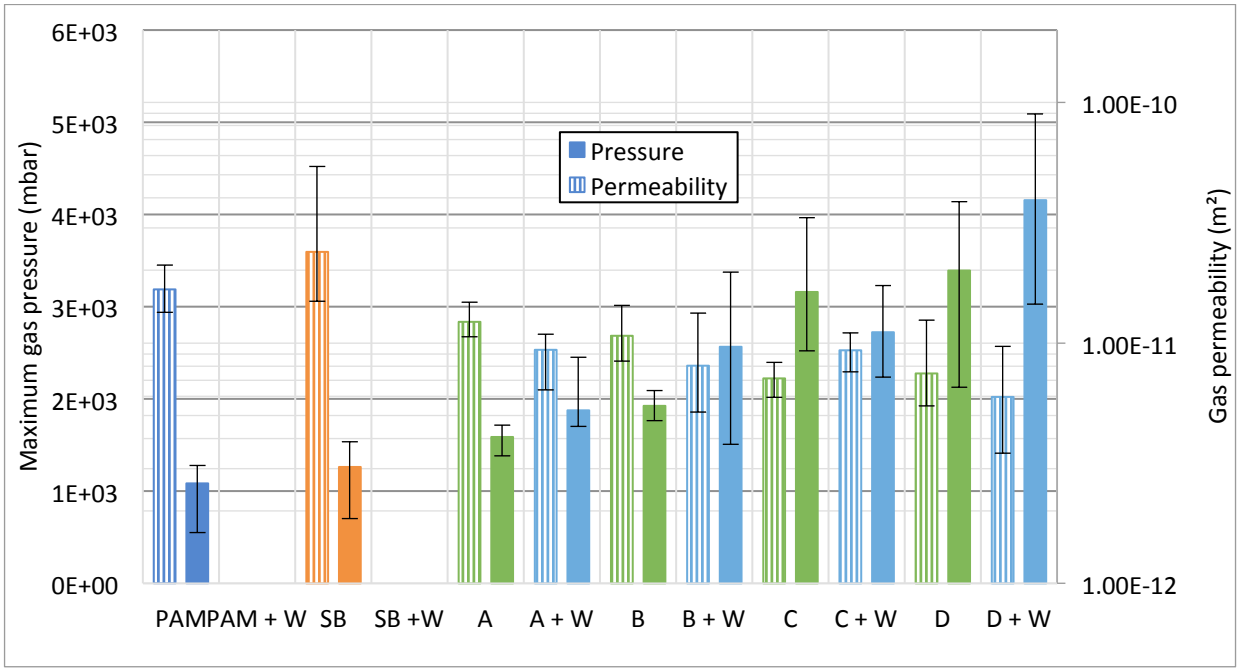

Figure 3. P_{max} and K_{gas} for PAM and new binders SB, A, B, C and D without and with injection of water (+W) before fluidization. Curing at 70 °C for 24 h followed by 6 days at 20 °C. Mean value on four samples and minimum/maximum error bar.

When tested without water injection, new binder SB has a similar P_{max} to PAM, but K_{gas} is 1.5 time higher than PAM. For binders A to D, P_{max} is 1.5 to 3.1 times greater than PAM, and permeability is 1.3 to 2.2 smaller than PAM. After water injection, PAM and binder SB have no more mechanical strength: sand is ejected of the tube at the initial flowrate of 1 ln/min. Binders A to D strengthen the compacted sand.
These first results show that, for the new binders A-D, despite improved water resistance and strengthening, K_{gas} .decreases significantly.

In order to preserve permeability, two new binders have been designed and tested (E and F) with m2 and m3 maturation processes (Figs. 4 and 5 respectively).
After maturation m2, without water injection before fluidization, P_{max} of binder SB is 1.5 smaller than PAM, whereas binders E and F have similar P_{max} to PAM. Correspondingly, K_{gas} of SB, and of binders E and F, is around two times higher than for PAM. With water injection, all samples consolidated with PAM and SB and one of the three samples consolidated with E fail during experiment, while all other samples consolidated E and F remain strengthened.

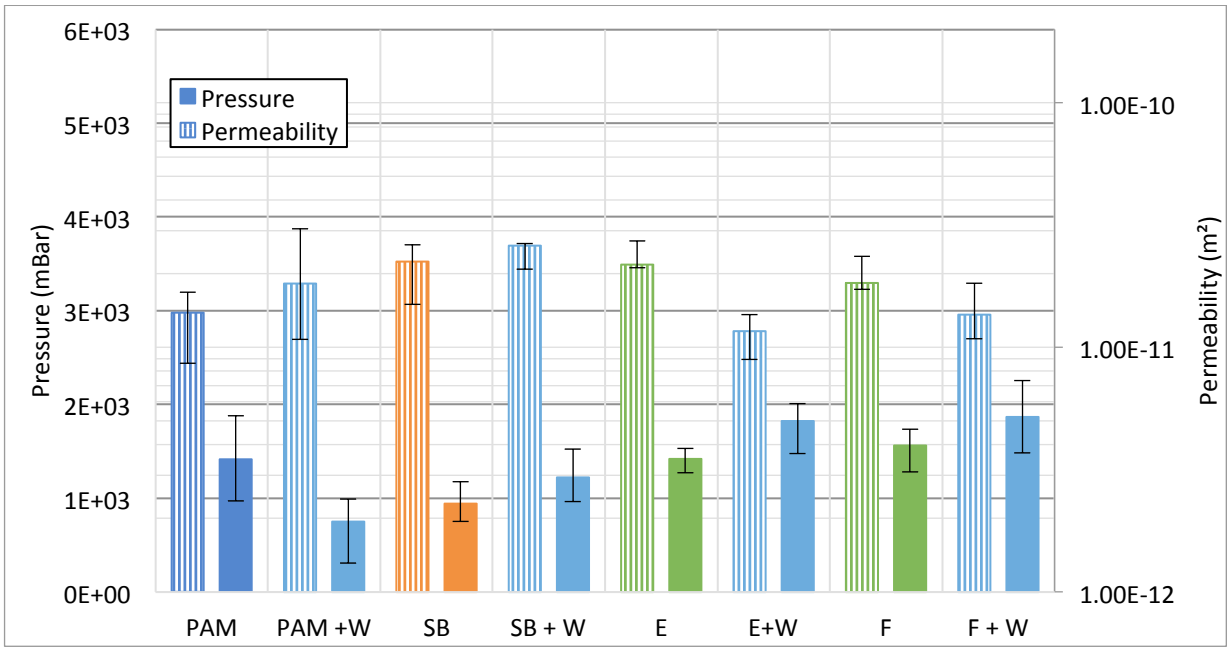

Figure 4. Maximum gas pressure and gas permeability for PAM and new binders SB, E and F without and with water injection before fluidization (+W). Maturation m2 is at 70 °C for 24 h followed by flushing, then 7 days at 70 °C. The mean value is over three samples (two samples for F+W) and minimum/maximum error bars are given. For one PAM sample, 3 PAM+W samples, one SB sample, 3 SB+W sample and one E+W sample, maximum gas pressure is failure pressure, for all others, Pmax is gas pressure at 15 ln/min (no failure).

New binders E and F do not induce a decrease in K_{gas}, and display a P_{max} similar to PAM. Moreover, their performance with water injection before fluidization is not degraded.

Concerning maturation m3 (at 20°C), without water injection, samples consolidated with PAM, SB and F have a similar P_{max}, while samples consolidated with binder E have a two

times higher P_{max}. Samples consolidated with PAM or E have two times smaller K_{gas} than samples consolidated with SB or F. After water injection, all the samples fail during the experiment.

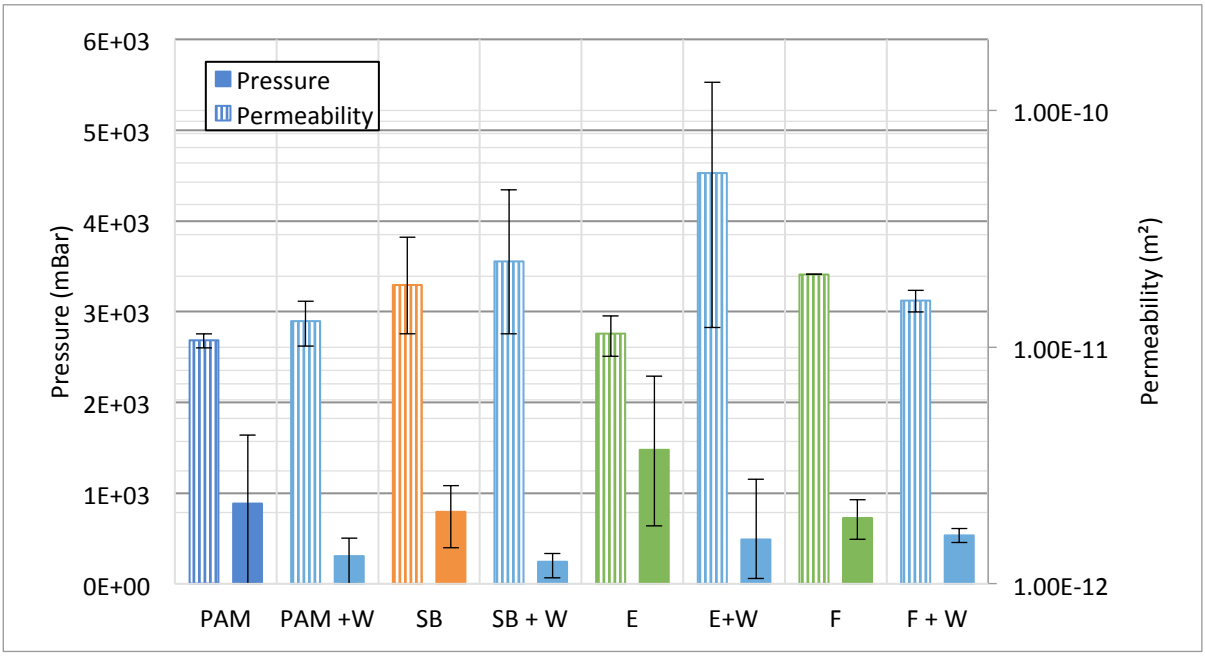

Figure 5. Maximum gas pressure and gas permeability for PAM and new binders SB, E and F without and with water injection before fluidization (+W). Maturation m3 corresponds to curing at 20 °C for 24 h followed by flushing, then 7 day at 20 °C. Mean values are for three samples (two samples for F+W) and error bars correspond to minimum and maximum values. For one SB sample and one E sample Pmax = pressure at 15 ln/min without failure, for all others samples Pmax = failure pressure.

The effect of maturation temperature is significant. Indeed, without water injection, samples cured with m2 method (at 70 °C for 8 days), samples withstand up to 15 ln/min, whereas samples cured with m3 (at 20°C for 8 days) fail before the experiment limit. After water injection, samples consolidated with binders E and F withstand after m2 maturation (70°C), but fail after m3 maturation (20°C).
Moreover, samples consolidated with PAM and SB show a better water resistance after maturation process m2 and m3 than after maturation process m1. The time lapse between injection and flushing is therefore a first order parameter for consolidation.

To sum up, new binders E and F strengthen porous media without decrease in K_{gas} independently of the maturation process (m2, m3). E and F induce a better resistance to water than PAM.

CONCLUSION

Seven new binders for chemical reservoir consolidation have been tested and compared to a reference polymer binder (PolyAcrylaMide PAM). The results obtained show a similar

strengthening to PAM, independently of maturation process. However, they present a better water resistance than PAM while preserving the reservoir permeability. The performances of all binders tested (PAM and NB) increase with the maturation temperature (here 20 or 70°C). New maturation process are currently tested to improve efficiency of new binders at 20°C.

ACKNOWLEDGEMENTS

Storengy is gratefully acknowledged for funding this research.

REFERENCES

[1] Hu C., "Etude expérimentale de propriétés mécaniques, de transport et poro-mécaniques d'un grès à haute porosité", *PhD Thesis*, (2017) Ecole Centrale de Lille, France.
[2] Carlson J., D. Gurley, G. King, C. Price-Smith, F. Waters, "Sand control: Why and How ?", *Oilfield Review*, (1992) **vol. 4**, 41-53.
[3] Moreno F. E., A. Rico, Z. Mendez, "New sand consolidation technique using hot alkaline solutions: laboratory Evaluation", *Canadian International Petroleum Conference*, (2002), paper 2002-122.
[4] Dees J. M., P. J. Handren, "A new method of overbalanced perforating and surging of resin for sand control", *Journal of Petroleum Technology*, (1994) **vol. 46**, 431-435.
[5] Zaitoun A., T. Pichery, "New polymer technology for sand control treatments of gas storage wells", *Society of Petroleum Engineers*, (2009), SPE-121291-MS
[6] Zaitoun A., R. Tabary, D. Rousseau, T. Pichery, S. Nouyoux, P. Mallo, O. Braun, "Using microgels to shut off water in a gas storage well", *Society of Petroleum Engineers*, (2007), SPE-106042-MS.
[7] Burrafato G., E. Pitoni, G. Vietina, L. Mauri, L. Chiappa, "Rigless WSO Treatments in Gas Fields. Bullheading Gels and Polymers in Shaly Sands: Italian Case Histories", *Society of Petroleum Engineers*, (1999), SPE-54747-MS.
[8] Gravelle A., "Optimisation de l'efficacité et de la durabilité des traitements de puits à base de polymères et de microgels dans un contexte de réduction de venues de sable", *PhD Thesis*, Institut National Polytechnique de Lorraine (2011), France.
[9] Sidiropoulou M. G., Moutsopoulos, K. N., Tsihrintzis V. A., "Determination of Forchheimer equation coefficients α and β", *Hydrological Process*, (2007) **vol. 21**, 534-554.
[10] Münch, B., Holzer, L. "Contradicting geometrical concepts in pore size analysis attained with electron microscopy and mercury intrusion", *J. Am. Ceram. Soc.* (2008) **vol. 91** (12), 4059-4067.